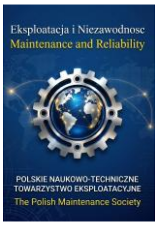

Eksploatacja i Niezawodnosc - Maintenance and Reliability

Volume 29 (2027), Issue 2

https://ein.org.pl

The Polish Maintenance Society

Evaluation of the efficiency of fuel cell vehicle in real driving conditions

Piotr Pielecha[1], Ireneusz Pielecha[1,*]

[1] Faculty of Civil and Transport Engineering, Poznan University of Technology, Poland

* Corresponding Author: ireneusz.pielecha@put.poznan.pl

Received: 21 April 2026
Revised: 2 July 2026
Accepted: 24 August 2026
Online: 1 September 2026

Abstract

The trend towards zero-emission vehicle propulsion results in a fuel cell system working in conjunction with an electric motor and battery system. The research carried out in this study concerns the evaluation of fuel cell performance made without any interference to the drivetrain. The article aims to fill a gap in research on the efficiency of fuel cells vehicle using a non-invasive method in real traffic conditions, which is lacking in the literature. The research was conducted using a 128 kW FCHEV (Fuel Cell Hybrid Electric Vehicle) under typical traffic conditions. As part of the work, the propulsion efficiency was determined for each driving phase. The following fuel cell efficiency values were obtained in the urban, suburban and highway phases: 51, 56 and 66% respectively. The values obtained are very close to the direct tests, while completely eliminating the need to modify the powertrain in order to determine the fuel cell efficiency.

Keywords: *hydrogen fuel cell, fuel cell indicators, real driving conditions, fuel cell efficiency*

Article citation:
Pielecha P, Pielecha I, Evaluation of the efficiency of fuel cell vehicle in real driving conditions, Eksploatacja i Niezawodnosc – Maintenance and Reliability 2027: 29(2) http://doi.org/10.17531/ein/231651

Highlights

- Analysis of FCHEV fuel cell efficiency without additional measurement systems.
- Cell efficiency determined on the basis of thermodynamic values.
- Fuel cell efficiency evaluated under real driving conditions.
- Higher fuel cell efficiency on highways than in urban conditions.
- Fuel cell efficiency ranges from 51% to 66% in different driving conditions.

1. Introduction

Hydrogen as an energy carrier fits perfectly into the trend towards decarbonisation in many sectors of the economy today, including the transportation sector in the EU (European Union) and worldwide. It is one of the strategic pillars introduced in the hydrogen strategy document introduced by the EU in 2020 and the Alternative Fuels Infrastructure Regulation. As a fuel, hydrogen has one key advantage – it does not generate CO_2 emissions directly. As such, it can play a key role in meeting the EU's climate neutrality target by 2050 [1,2]. However, despite proactive EU action, FCHEVs (Fuel Cell Hybrid Electric Vehicles) represent a minor share of the total vehicle fleet. The insignificant amount of FCHEVs in the total vehicle share is linked to the low availability of this type of powertrain.

According to the European Alternative Fuels Observatory, 6441 hydrogen-powered vehicles were on the roads in Europe in Q2 2025. According to the United Nations document on the classification of road vehicles [3] among these, 5393 are N1 and M1 category (vehicles with no more than 8 seats and not exceeding 3.5 tonnes), 637 M2+M3 passenger vehicles (exceeding 3.5 tonnes) and 411 N2+N3 (goods carrying vehicles exceeding 3.5 tonnes) can be differentiated. From 2012 to 2022, the year-on-year increase in the number of vehicles was around 40%. In 2023 and 2024, it decreased to around 5% [4].

In Europe, Germany has the highest number of FCHEVs registered with 2063 vehicles. The second largest market in Europe is France and the Netherlands third with 1301 and 778 units respectively. The United Kingdom, Poland, Switzerland and Norway each have around 450 FCHEVs registered. In the remaining 16 countries, the total number of FCHEVs does not exceed 125. There are still some countries in Europe where not a single FCHEV is officially registered [4].

In 2017, the total number of FCHEVs worldwide was only 7186 vehicles [5]. By the end of 2021, this number increased to 51,437 [6]. On the other hand, in 2024, their number exceeded 86,700 vehicles and is expected to exceed 100,000 in 2025 [7]. Figure 2 shows the share of each continent in total number worldwide.

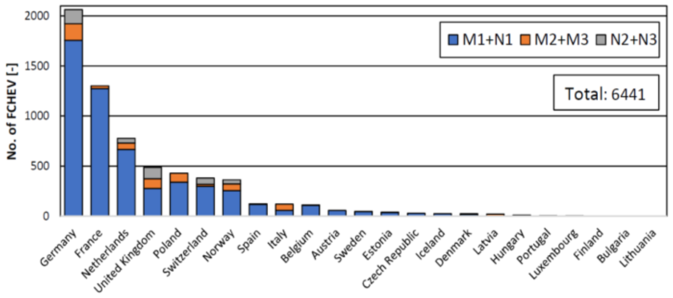

Figure 1. Number of FCHEVs registered in the country by vehicle category [4].

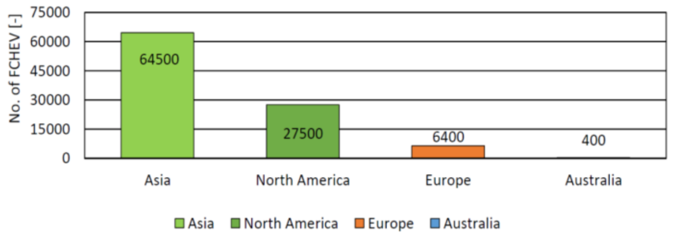

Figure 2. Number of FCHEVs in operation on each continent in 2025 [7].

The main market with the highest number of registered FCHEVs is Asia with a 65% share. North America represents 26% of the market and Europe just under 9%. The other continents have a marginal share.

In terms of passenger vehicles, South Korea is the largest market with a share of around 50% of the total FCHEV market worldwide and 80% in Asia. Japan is second in Asia with just under 20%, and China closes the market on the continent with a share of less than 1%. In North America, 98% of the market is accounted for by the USA, with Canada holding the remaining 2%. The European market was described earlier. The Australian market accounts for only 0.4% of the global share of FCHEVs [6].

The Asian market, compared to the European and USA (United States of America) markets, is characterised by different regulations, which not only actively promote hydrogen as a fuel, but at the same time are not as restrictive. An example of this is the wider choice in vehicle manufacturer offerings in the Asian market. Countries like Japan have set a target of 800,000 FCHEVs on the roads by 2030 and China as many as 10,000,000 by 2035 [8].

Such a small number of hydrogen vehicles is mainly due to their low availability, high cost of purchase and operation and an undeveloped hydrogen refuelling station infrastructure. In 2020, there were 553 HRS (Hydrogen Refuelling Stations) worldwide, with more than 200 in Europe – including around 100 in Germany, 275 in Asia only 75 in North America [9]. In 2021, this number increases to 729 and in 2022 to 1022 in 31 different countries [6,10]. At the end of 2024, as Fig. 3 shows, the milestone of 1,000 HRS has been reached, and more precisely the number of 1160 stations available in 45 countries worldwide has been reached [11,12].

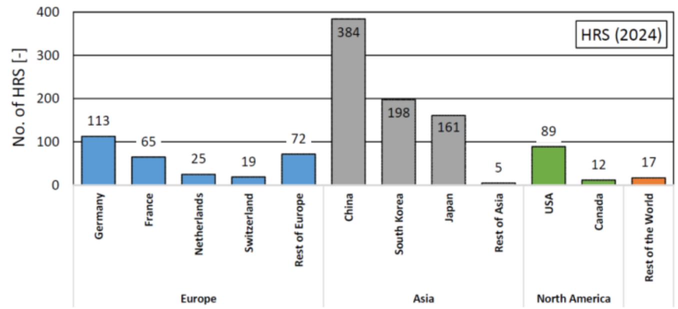

Figure 3. Number of HRS (Hydrogen Refuelling Stations) stations by country and continent [11,12].

In the coming years, the EU has obliged Member States to expand HRS infrastructure through Directive Regulation (EU) 2023/1804. According to it, along the main TEN-T (Trans-European Transport Network) corridors, HRS stations have to be available every maximum of 200 km or at every major urban node. Their characteristics and infrastructure must ensure the capacity to refill 1 tonne of hydrogen per day at a pressure of at least 700 bar. These targets have to be met by 2030 [2,13].

There is still a lack of comprehensive analyses of fuel cell efficiency under real-world FCHEV operating conditions in the literature. Previous studies have focused mainly on laboratory or dynamometer tests, which, despite their high repeatability, do not reflect the variability of loads, temperatures and operating dynamics characteristic of real-world traffic. At the same time, standard methods of measuring hydrogen consumption, based on flow meters or cylinder weighing, require direct interference within the vehicle's fuel system, which excludes their use in commercial FCHEVs. The real interest in the proposed methodology comes from the growing need to assess the efficiency of FCHEV vehicles in conditions that reflect actual operation, rather than just a laboratory or type-approval test environment. This results in a significant research gap: the lack of, non-invasive methods for accurately assessing fuel cell efficiency while driving in real road conditions. This paper addresses this issue by proposing an approach based only on values and parameters available in the vehicle's factory diagnostic system, without any modification to the powertrain.

2. Literature review

2.1. Analysis of overall powertrains efficiency

The energy efficiency of different powertrains in passenger vehicles has been one of the main topics of consideration in scientific articles in recent years. An increase in the efficiency of the propulsion system results in lower consumption of the energy carrier, as well as a reduction in exhaust emissions and indirect losses. In the literature, indicators such as Tank-to-Wheel (TtW), Well-to-Wheel (WtW) or Life Cycle Assessment (LCA) are often used to assess the level of energy efficiency.

Due to the nature of this paper, in the following analysis, the focus will be only on the efficiency of the power unit. Losses associated with the storage, transfer and processing of the energy carrier at earlier stages will be omitted. Only the process of direct conversion of the fuel supplied to the drive unit or fuel cell into mechanical or electrical energy used to power the vehicle will be considered.

Table 1. Evaluation of the overall efficiency (maximal) of modern drive systems.

Powertrain type/test type	η_o [%] – laboratory	η_o [%] – RDC test
ICE – SI	20–44 [14-17]	8–26 [18-20]
ICE – CI	25–47 [14,16 21]	16–42 [20,22]
BEV	50–97 [23-26]	50–96 [20,27]
FCHEV	66–68 (steady-state) [28,29]	–

Table 1 summarises the overall efficiency ranges of various typical powertrains in laboratory tests and in real road traffic conditions of passenger vehicles. Vehicles with ICE – SI (Spark-Ignition Internal Combustion Engines) have the lowest efficiency of all the propulsion types analysed. In laboratory tests, they operate with an efficiency ranging from several percent to a peak of about 35%. In real-life conditions, this efficiency operates in the range of 8–26%, according to [18-20]. In the case of vehicles with ICE – CI (Compression-Ignition Internal Combustion Engines), the values are slightly higher, with tests under laboratory conditions indicating values ranging from 25 to as high as 47% [16], and under actual operating conditions these values take on several percentage points lower values [20,22]. Electric motors in BEV (Battery Electric Vehicles) have significantly higher efficiency values. Their ranges in laboratory and road tests range from about 50 to 97% [20,23-27]. A deficit of research results on FCHEV-type powertrains can be found in the literature. According to [29], the efficiency of an FCHEV in laboratory tests is 66.8%, and in a laboratory test reflecting UDDS (Urban Dynamometer Driving Schedule) urban driving, the efficiency of the FCHEV powertrain was 67.7% [28].

2.2. Fuel cell power analysis

Hydrogen storage methods do not affect its lower heating value (120 MJ/kg); however, temperature is a significant factor in terms of its density: 0.0987 kg/m³ (at 0°C – gaseous hydrogen); 70.85 kg/m³ (at –253°C – liquid hydrogen) and 858 kg/m³ (at –259°C – solid hydrogen) [30].

Manufactured fuel cell automotive vehicles use cells with power outputs in the range 95–130 kW: 114 kW (Mirai 1st gen.) [31], 128 kW (Mirai 2nd gen.) [32], 103 kW (Honda Clarity) [33], 95 kW (Hyundai Nexo) [29], 115 kW (Saic MAXUS FCV80) [34].

The fuel cells used in the first prototype vehicles (in 2002) achieved a volumetric power rating of 1.5 kW/dm^3 with a mass power rating of 0.75 kW/kg [35]. In the Toyota FCHV-adv model (in 2008), these ratios were 1.45 kW/dm^3 and 0.9 kW/kg, respectively. The first generation Toyota Mirai had values of 3.0 kW/dm^3 and 2 kW/kg respectively. The second generation has values of 5.4 kW/dm^3 [32] and 5.4 kW/kg (4.4 kW/kg including end plates) [36].

The Hyundai Nexo FCHEV has achieved significant technological advancements compared with its predecessor, the Tucson ix35: improved system efficiency from 55% to 60% [37]. The Hyundai Nexo reports a power-to-volume ratio of 3.1 kW/dm^3 [38].

Honda used fuel cells in the Clarity for which the volumetric and mass power ratios were, respectively: 3.1 kW/dm^3 and 2.0 kW/kg [33,39].

The cost of platinum is assumed to be around 40–55% of the cost of the fuel stack [40]. The first fuel cell systems (Gemini space in 1962) contained very high amounts of platinum (35 mg/cm^2) while generating low current values (37 mA/cm^2) [41]. Recent decades bring a significant reduction in the use of platinum in fuel cells. It has been reported that the use of platinum in a fuel cell has decreased from 1.0 mg/cm^2 in 2002 to 0.365 mg (anode loading of 0.05 mg/cm^2 and cathode of 0.315 mg/cm^2 [42]) in 2016 (Toyota Mirai I) to a value of 0.125 mg/cm^2 in fuel cell test systems [43-45]. The platinum content of the 2nd generation Toyota Mirai is approximately 19.2 mg/cm^2 (27 g of platinum was contained in the 1st generation Toyota Mirai cell).

2.3. Analysis of cell performance evaluation options: indirect and direct

Direct methods are recommended for measuring hydrogen consumption. These are covered by ISO 23828 and SAE J2572 standards [46,47]. The recommended methods are: the weight method and the hydrogen flow method. Both of these methods were omitted in this study: the first method requires the use of an external hydrogen tank system, while the second requires interference in the hydrogen supply system, which was not allowed.

Current (indirect) methods of measuring hydrogen consumption in vehicles can be divided into five groups [28,29,48]:

a) Current-based: instantaneous measurement,
b) Tanks pressure and temperature, using IR (Infrared)-read values,
c) Tanks pressure and temperature, using CAN (Controller Area Network) values,
d) The O_2 method,
e) Vehicle dashboard display information (direct reading).

The first method relates to the direct correlation between the current flowing through a single cell in the stack and the corresponding amount of hydrogen flowing (with a known number of cells):

$$\dot{m}_{H_2} = \frac{I_{st} \cdot N_{cell} \cdot M_{H_2}}{nF} \quad (1)$$

where: M_{H_2} [g/mol] the hydrogen molar mass, n the number of mole of electron per mole of H_2 consumed, F [C/mol] the Faraday constant, I_{st} [A] the stack current and N_{cell} the number of cells.

The second method involves the use of an infrared sensor to determine pressure and temperature. Unfortunately, the measurement is only taken when the vehicle is stationary (refueling), which allows for a differential result to be obtained. It is possible to calculate the normative fuel consumption in accordance with the measurement method specified in SAE J2572 [46].

The third method involves the use of an equation that takes thermodynamic conditions into account:

$$P \cdot V = Z \cdot m_{H_2} \cdot R \cdot T \quad (2)$$

where: T [K] being the equivalent hydrogen temperature in tank, m_{H_2} [kg] the hydrogen mass trapped into the tank, V [m^3] the volume, P [Pa] the tank pressure, Z [-] the compressibility factor. The compressibility factor Z was determined from the following equation, which was analytically obtained based on the data points in the table included in UN Regulation No. 154 containing regulations on the homologation of FCHEV vehicles [49]:

$$Z = 0.28789 \cdot 10^{-4} + 0.26626 \cdot 10^{-2} \cdot T + 0.56502 * 10^{-2} \cdot P - 0.58298 \cdot 10^{-6} \cdot T^2 - 0.15022 \cdot 10^{-4} \cdot T \cdot P - 0.41998 \cdot 10^{-5} \cdot P^2 - 0.90709 \cdot 10^{-8} \cdot T^3 + 0.22222 \cdot 10^{-7} \cdot T^2 \cdot P + 0.234251 \cdot 10^{-8} \cdot P^3 \quad (3)$$

The error committed when using equation (2) relates to the “accuracy” of the hydrogen pressure and temperature measurements. Typical measurement errors are 0.5% FS (maximum) for hydrogen pressure and 0.1°C (maximum) for temperature. A temperature drop of 0.1°C causes the calculated mass to increase by 1.5 g (at a maximum tank pressure of 69 MPa). A pressure change of 0.1% causes a mass change of 0.85 g. In the worst-case scenario (cumulative errors), a mass determination error in the range of 2–3 g is obtained.

The equation allows for an R^2 fit value of 0.999 in the temperature range of 280–292 K and pressure range from 50 to 70 MPa. These values are the boundaries of these parameters during data acquisition in a test under real road conditions.

The fourth method is based on measuring the oxygen concentration, pressure, and temperature in the exhaust system. Knowing the oxygen consumption, it is possible to determine the hydrogen consumption. This method (like the first method) does not take into account blow-by and hydrogen leakage.

The relative differences between the four methods (without the O_2 method) of measuring hydrogen consumption in the WLTC (Worldwide Harmonized Light Vehicles Test Cycles) test are presented in [48]. The analysis of the studies shows that the smallest error (3.2%) is made in the last method (Vehicle dashboard display information), while the largest error is made when using an IR sensor (28.8%). This is due to the fact that this method allows the measurement of hydrogen pressure and temperature – as previously stated – only when the vehicle is stationary, i.e., at the beginning and end of the test.

2.4. Assessment of automotive fuel cell efficiency

The rapidly growing market for fuel cell vehicles means that research on fuel cells in vehicle systems is becoming increasingly carried out. The research conducted by Duan et al. [50] on two different types of FC (Fuel Cell) vehicles involved stationary or dynamometer testing. A hydrogen flow meter was installed in the system and the method of measuring the pressure and temperature of hydrogen in the tank was used. Specific measurement methods allowed only the assessment of hydrogen consumption per unit of energy (which is difficult to compare in the case of road tests).

The remaining works (Table 2) concerned the precise determination of fuel cell efficiency. Unfortunately, these tests were always conducted in a laboratory setting, which, as is well known, does not accurately reflect typical traffic conditions. The studies used additional measuring devices (hydrogen flow meters) which are not fitted as original equipment in vehicles.

Table 2. Analysis of fuel cell performance evaluation conditions.

Bibliography	FC efficiency	Specification	Instrumentation
Lohse-Busch et al. [28]	66% (max)	Test NEDC (Mirai II)	Micro Motion™ Coriolis hydrogen mass flow meters (low flow range CMF010 M and high flow range CMF025M
	67.7%	Test UDDS (Mirai II)	
	57.1%	Test US06 (Mirai II)	
Sery et al. [29]	66.8% (max)	Steady-state (Nexo)	Indirect measurement without hydrogen flowmeter

3. Purpose and scope of research work

The subject of fuel cell efficiency in means of transport has not been fully explored. Due to their dynamic changes, a specific assessment of efficiency is required. Static load testing of fuel cells allows for a relatively quick estimation of their efficiency [51]. Research is also being conducted on estimating efficiency under constant driving conditions [52] or simulations of driving test conditions [53]). However, these are still not typical conditions for a vehicle equipped with a fuel cell powertrain.

The authors have determined the hydrogen consumption of a hydrogen-powered vehicle under typical driving conditions. Until now, fuel consumption figures under various driving conditions were not known. Furthermore, using this data, the efficiency of fuel cells under these conditions has been determined. Until now, the focus has been on the maximum efficiency of fuel cells, rather than on efficiency values under various driving conditions.

There are only few research results in the literature on this subject [28,48] concerning the assessment of fuel cell efficiency in FCHEV passenger cars in real or near-real traffic conditions. Many articles focus on laboratory tests using indirect and direct methods. Therefore, the main objective of the conducted research is to evaluate the efficiency of the fuel cell stack of an FCHEV passenger car in real traffic conditions without directly interfering in the vehicle's drive system.

The scope of the study was divided into three segments: urban, suburban, and highway driving conditions. This allowed for the verification of energy efficiency in the context of variable driving characteristics and dynamics.

The tests were characterized by no interference with the vehicle's drive system, and no additional flow meters or sensors were installed. The analysis was carried out using the third indirect method described above, analytically based on physical laws. The vehicle's efficiency was determined using readings from the available sensors originally located in the vehicle.

4. Research methodology

4.1. Research object

Research on fuel cell performance was conducted by using the Toyota Mirai II. The vehicle's technical data, with particular emphasis on fuel cells, is presented in Table 3. In addition, a comparison with the previous generation was made.

The diagram of the vehicle's drive system used for testing is shown in Fig. 4, which also indicates the measured values for determining the efficiency of fuel cells. The main measured values are fuel cell parameters and hydrogen consumption parameters based on thermodynamic changes in hydrogen contained in composite tanks.

Table 3. Technical specifications of Toyota Mirai II fuel cells [36].

Vehicle	Unit	Toyota Mirai II
Power	kW	128
Hydrogen storage capacity	kg	5.6
Number of cells	–	330
FC volume	dm^3	24
FC mass	kg	24
Cell thickness	mm	1.11
Thickness of separator	mm	0.1
Number of flow channels	–	2
Vol. power densities (excl. end plates)	kW/L	5.4
Mass power densities (excl. end plates)	kW/kg	5.4

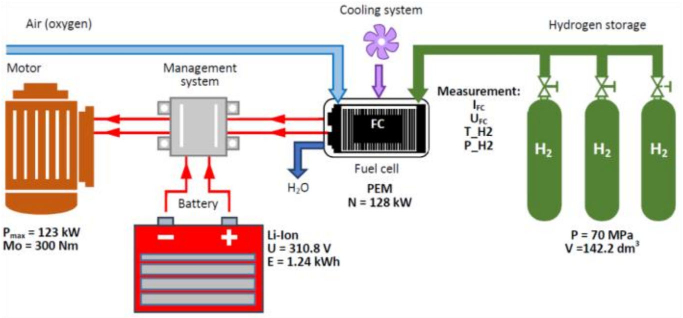

Figure 4. Schematic of the Toyota Mirai II drive system.

4.2. Measuring equipment

The study used a dedicated TechStream by Toyota data acquisition device to record data from two controllers: the FC controller and the EV controller. In total, over 400 measurement data points were acquired, resulting in a data recording frequency of 0.14 Hz (Δt was approximately 7 s). The low sampling rate was due to the large number of parameters being recorded. Using a dedicated CAN data logging system, a complete data set was acquired. This resulted in a low sampling rate, but enabled the recording of a large volume of data, the analysis of which contributed to a better understanding of the powertrain's operation. Out of all the measured parameters, the most important ones used for further analysis were time, vehicle speed, cell voltage, battery voltage, battery current, fuel cell current, fuel cell voltage, and SOC. Nevertheless, the most important parameters for determining efficiency were the pressure and temperature in the vehicle's high-pressure hydrogen tank. Based on this input data, it was possible to analytically determine the remaining values shown later in this article.

All parameters related to additional equipment that increases the vehicle's hydrogen consumption, such as air conditioning, heated seats, and satellite navigation, were omitted because they were purposely turned off so as not to affect the results of this analysis. During the test, the vehicle operated in the default drive system settings mode.

4.3. Scope of research

The tests in real traffic conditions were carried out in accordance with the requirements of the RDC (Real Driving Condition) test, which are also presented in Fig. 5. The tests show that the basic parameters have been met (other values, such as the contributions of speed and acceleration, were not presented, as they were also met and are not particularly relevant here). The tests lasted 103 minutes (exactly 7234 seconds), which means that this requirement was also met (the RDC test should last between 90 and 120 minutes). Each phase (except for the urban phase) lasted almost exactly as long as recommended by the RDC test (without additional deviations). Taking these variations into account means that the length of the urban phase is also correct. The test is shown in Fig. 5 included urban driving in the first part (average speed of 26.5 km/h), followed by sub-urban driving (average speed of 66.2 km/h) and highway driving (average speed of 112.3 km/h).

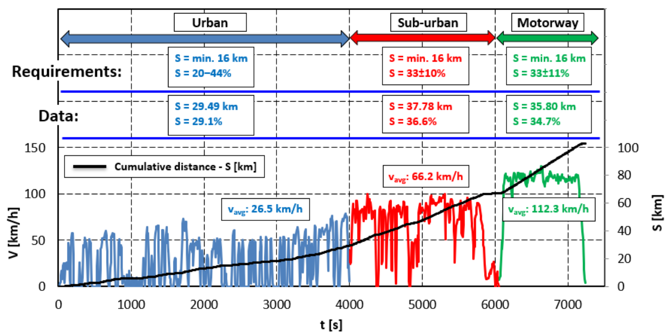

Figure 5. The course of the RDC (Real Driving Cycle) research test was divided into driving phases (additionally required driving phase intervals and actual values), average speed in individual test phases, and cumulative test distance.

5. Fuel cell testing under road conditions

5.1. Voltage-current characteristics of a fuel cell stack

The analysis of the fuel cell stack operating conditions is presented in Fig. 6. The voltage-current characteristics indicate that a large share of the cell's operation occurs at power values less than half of the maximum value. This means that the cell operates at a voltage U above 225 V (it means that a single cell generates above 0.68 V). It is important to note that the minimum voltage is not lower than 0.5 V (exactly U_{min} = 183/330 = 0.55 V), which means that losses resulting from mass transport are almost non-existent [54,55]. Activation losses are quite significant – this is due to the fact that the cell voltage without load should be around 330 V. In the analyzed case, there is a drop of 0.12 V on a single cell (the maximum voltage of a single cell without load is U_{max} = 0.88 V).

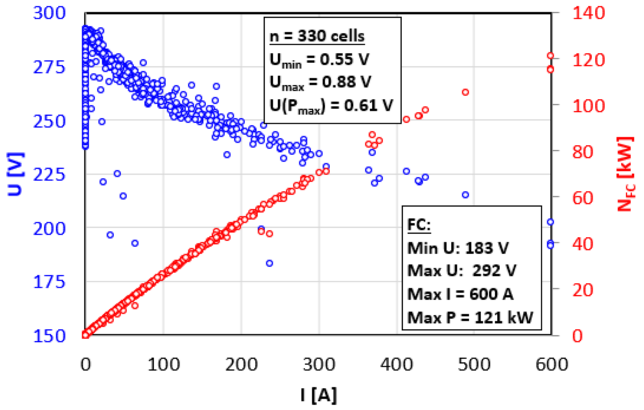

Figure 6. Voltage-current characteristics of a fuel cell with typical operating values.

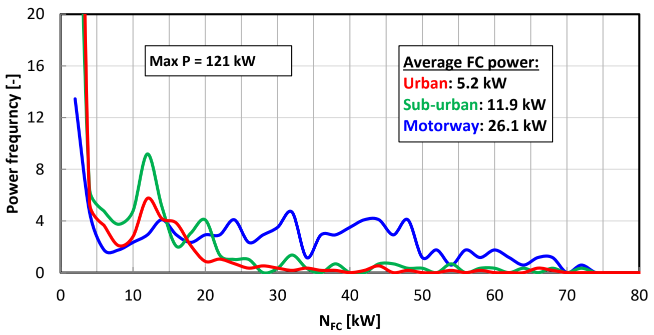

(a)

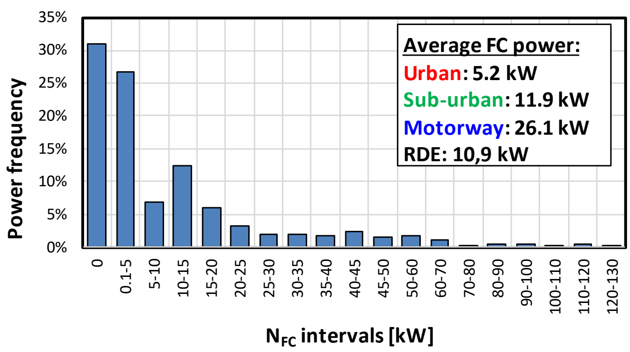

(b)

Figure 7. Frequency of power of fuel cell (FC) occurrence in individual driving modes in the RDC test (a) together with average power values in individual test phases (b).

5.2. Fuel cell stack power analysis

The analysis of power frequency in each phase is presented in Fig 7a. It shows that in urban conditions, cell power below 5 kW was most commonly used. Apart from minimum power, the most common value is in the range of 10–15 kW. During the non-urban phase, the dominant cell power range is also 10–15 kW, with twice the frequency of occurrence. In this phase, the value of approximately 20 kW is also significant, occurring quite frequently. In the non-urban phase, a much wider power range of 25–50 kW dominates. Figure 7b shows the total fuel cell power values by range. Idling has the largest share (over 30%), and the 0.1–5 kW range covers over 25% of the occurrence time. This means that fuel cell power up to 5 kW is used for half of the vehicle's driving time. The smallest share of low fuel cell power values was recorded in the highway phase (below 15%).

5.3. Thermodynamic analysis of hydrogen storage

Figure 8 shows the thermodynamic values for hydrogen storage. The pressure values at each stage of hydrogen reduction are shown in Fig. 8a. It shows that the total pressure change in high-pressure tanks (stage 1) during the tests was 18.96 MPa. Difference is due to the natural consumption of hydrogen during driving. The reduction in hydrogen pressure (stage 2) is constantly maintained, as evidenced by the very small pressure change of 97 kPa (only 7.7% of the average value). Large pressure differences were recorded at the last reduction stage (stage 3) – hydrogen injection into the fuel cell. The largest instantaneous differences occur during high fuel cell load, which is associated with high hydrogen consumption and the simultaneous operation of all three hydrogen injectors. The largest share of operating time is related to the use of one injector – 94.3%; two injectors operated 3.3% of the time; three – only 0.57%. There were also conditions in which no hydrogen was supplied to the cell: 1.7% of the vehicle's operating time.

The analysis of temperature changes in high-pressure tanks is shown in Fig. 8b. It shows that each tank has a different temperature. Therefore, the average value was determined (Fig. 8b) and the differences in each tank in relation to the average value were shown. The average temperature in the first tank is slightly higher than the average and is +0.8°C. The changes in the temperature are the greatest in the first tank. The temperature of the second hydrogen tank is very similar to the average value and the difference is about –0.03°C. The temperature in the third tank is the lowest, averaging –0.7°C less. Large drops in temperature in the three tanks (after approximately 6000 s) are caused by high hydrogen consumption under highway driving conditions.

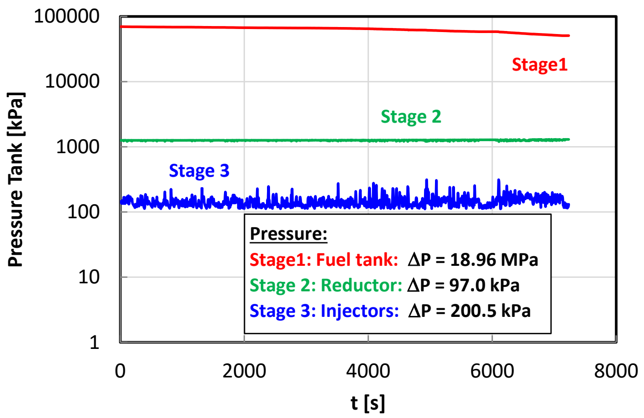

(a)

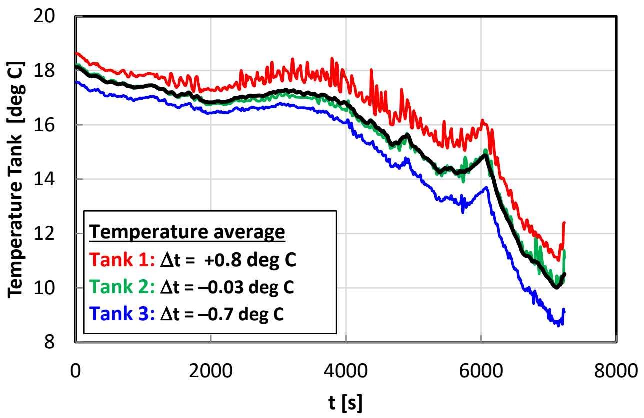

(b)

Figure 8. Characteristics of fuel pressure changes in high-pressure tanks and at each successive stage of hydrogen pressure change (a) – ΔP stands for the maximum change in fuel pressure in the tank during testing) and temperature in three high-pressure tanks (b); the figure shows the maximum deviation Δt from the average value (black line).

5.4. Assessment of hydrogen consumption under road conditions

A more detailed analysis of hydrogen consumption is presented in Fig. 9. In urban conditions, the power of the cells is low and the average hydrogen consumption is also not high, averaging 0.06 g/s. In non-urban conditions, the cell power is higher, and therefore hydrogen consumption is also more than twice as high, averaging 0.17 g/s. In highway conditions, the average power was again more than twice as high, which translates into an average hydrogen consumption of 0.36 g/s.

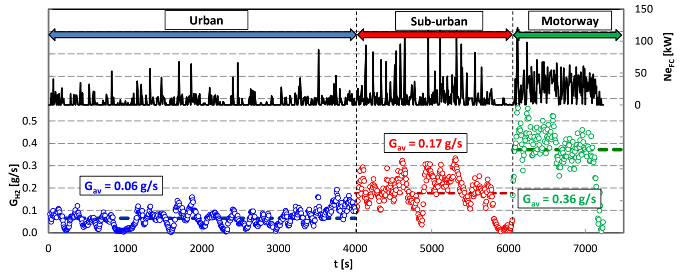

Figure 9. Hydrogen consumption values in each phase of the route.

Although the battery accounts for only a small proportion of the total power balance of a hydrogen vehicle (approximately 18% [56]), an analysis of its use is presented. In urban conditions, power consumption is approximately 20 kW, but braking doubles this value to approximately 40 kW (Fig. 10). In sub-urban driving conditions, it is approximately 25 kW, and braking still achieves a higher value: up to 40 kW of recovered power. In highway driving conditions, it is quite similar: the battery power is 25 kW, and the power recovery is also 40 kW. A comparison of all battery operating conditions shows that high power recovery occurs mainly during braking in urban and sub-urban phases. The lack of high braking power values in the highway phase is mainly due to the lack of braking.

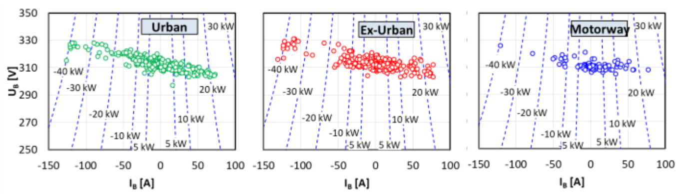

Figure 10. Current-voltage characteristics of the battery divided into driving phases.

In accordance with equation (3), the spatial path of changes in the Z factor, taking into account the compressibility of hydrogen, was determined. When the pressure changes in the range of 50–70 MPa and the temperature in the range of 10–18°C, the Z factor changes in the range of 1.36 to 1.45 (higher values are obtained at higher pressures and lower temperatures). Figure 11 shows the spatial interpolation of the Z coefficient values based on data contained in the document concerning the type homologation of FCHEV vehicles [49]. The graph on the left shows all values of the Z parameter within the temperature range of 50–350 K and the pressure range of 0–80 MPa. The area in red indicates the temperature and pressure ranges encountered during the road test. On the right-hand side the red zone has been expanded and the points showing changes in parameter Z has been added. The black marks indicate the values of the Z factor during the test. The irregularity of the changes results from periodic higher hydrogen consumption values, which could be seen as a drop in pressure in the tank and a certain inertia of temperature changes following consumption.

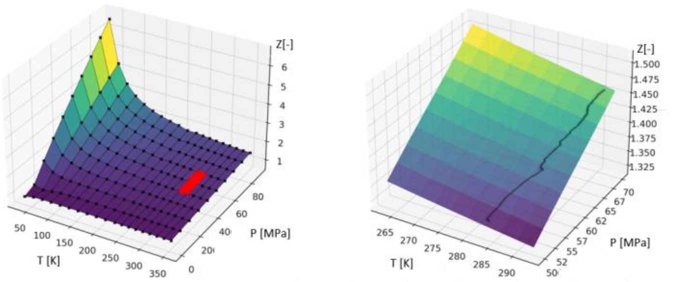

Figure 11. Spatial characteristics of the Z factor and its trajectory during the test.

Based on equation (2) and taking into account the compressibility factor Z (equation 3), hydrogen consumption values were determined for each driving phase (Fig. 12). In urban conditions, consumption was 0.26 kg, which corresponds to 0.90 kg/100 km during an urban route. In non-urban conditions, the cell power output is higher, which increases hydrogen consumption. In the non-urban phase, it was 0.36 kg, which corresponds to a consumption of 0.96 kg/100 km. The highway phase requires high power output, which results in high hydrogen consumption: 0.44 kg (the hydrogen consumption per kilometer was 1.24 kg/100 km). Taking into account three phases of driving allows for the assessment of average hydrogen consumption during the route covered: 1.03 kg/100 km. This value is very close to the value declared by the manufacturer and obtained in a different test. This means that the RDC test is similar to the homologation conditions.

As shown above, the energy consumption values were not analyzed, as it was necessary to include the battery energy (not only consumed but also recovered during regenerative braking) in this balance.

Determining hydrogen consumption and knowing the power generated by fuel cells made it possible to evaluate the efficiency of fuel cells. Due to non-monotonic hydrogen consumption readings in the vehicle's diagnostic system, the pressure in the high-pressure tank was averaged and the temperature read from these tanks was averaged simultaneously. The resulting analysis of the energy used by the fuel cells at one-minute intervals in each phase was performed, and the average values of this energy in each phase were determined. The results of this work are presented in Fig. 13.

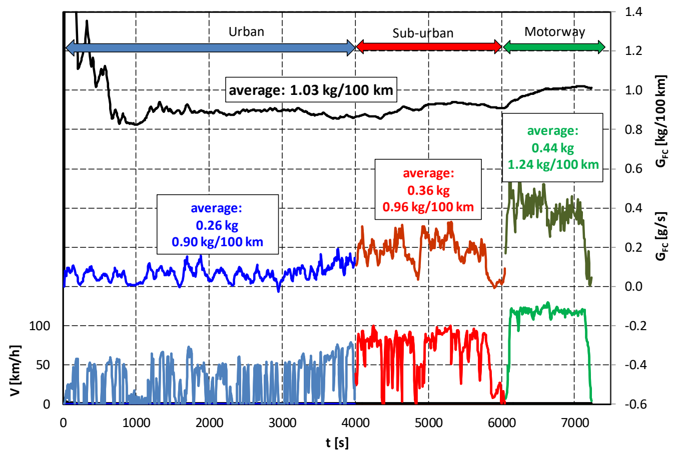

Figure 12. Hydrogen consumption values during driving phases.

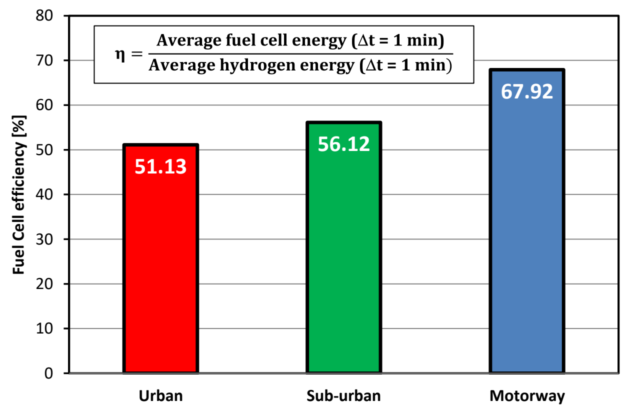

(a)

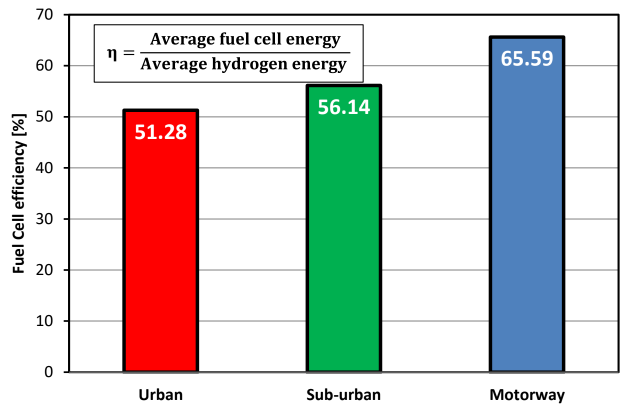

(b)

Figure 13. Analysis of fuel cell efficiency in a vehicle during a driving test: (a) determined at 1-minute intervals in each phase; (b) averaged over the entire period of each driving phase.

It shows that in 1-minute intervals (Fig. 13a), the lowest cell efficiency was achieved in the urban phase – 51.13%. In the sub-urban phase, the efficiency was higher and reached 56.12%. In the highway phase, the cell power is the highest and the efficiency also reaches values of up to 67.92%. The average for the full phases (Fig. 13b) shows slightly higher efficiency values in the urban and sub-urban phases (51.28% and 56.14%, respectively). In the highway phase (due to the even speeds), the efficiency for the entire phase dropped to 65.59%.

As can be seen from the above data, the interval and full-phase efficiency differ by less than 1% in urban and sub-urban phases and by approximately 3.5% in the highway phase.

5. Conclusion

Fuel cell efficiency stack tests were performed using a second-generation Toyota Mirai under road test conditions. Diagnostic data from the vehicle was used for the tests. Cell efficiency analyses were based on changes in hydrogen pressure in high-pressure tanks while driving.

The analysis of fuel cell efficiency under road test conditions leads to the following conclusions:

1. Due to the lack of a typical hydrogen flow meter (fitted as standard on the vehicle), hydrogen consumption and cell efficiency are determined indirectly. Such actions affect the estimation of fuel consumption and system efficiency.
2. Hydrogen consumption was analyzed in 1-minute intervals and in full test phases. Fuel consumption and cell efficiency values were determined in each phase. Fuel consumption is relatively proportional to vehicle speed conditions in each phase. Given that FC accounts for over 80% of the vehicle's propulsion [56], hydrogen consumption is a good indicator of vehicle speed. In urban conditions, hydrogen consumption is 0.90 kg/100 km. In non-urban conditions, hydrogen consumption increases, but does not exceed 7% (up to 0.96 kg/100 km). In highway conditions, hydrogen consumption increases by almost 30%. This is mainly due to driving speed.
3. Efficiency analysis shows that cell efficiency increases with driving speed (vehicle load): in urban conditions it is 51.2% (averaged) and 51.1% in minute intervals; in sub-urban conditions: 56.1% and 56.1% respectively; under highway conditions, efficiency is highest, at 65.6% throughout the entire phase and 67.9% in the interval analysis.

Considering the irregular pressure changes in the high-pressure system (and the inability to clearly determine hydrogen consumption), the following actions are recommended:

1. Analysis of hydrogen consumption and fuel cell efficiency stack under specific and constant driving conditions.
2. The analyses should cover different driving speeds in order to determine a wide range of cell loads.
3. Constant driving conditions will stabilize the temperature and pressure in the tanks, which will allow for a much more accurate determination of hydrogen consumption and fuel cell efficiency under actual driving conditions.

References

1. A hydrogen strategy for a climate-neutral Europe. Communication from the Commission to the European Parliament, the Council, the European Economic and Social Committee and the Committee of the Regions; 2020; Brussels. https://energy.ec.europa.eu/system/files/2020-07/hydrogen_strategy_0.pdf.
2. EU. Regulation (EU) 2023/1804 of the European Parliament and of the Council of 13 September 2023 on the deployment of alternative fuels infrastructure, and repealing Directive 2014/94/EU (Text with EEA relevance). Published online July 20, 2025. https://eur-lex.europa.eu/eli/reg/2023/1804/oj/eng.
3. Consolidated Resolution on the Construction of Vehicles (R.E.3). United Nations, Economic and Social Council, ECE/TRANS/WP.29/78/Rev.7, 2023. https://unece.org/transport/vehicle-regulations/wp29/resolutions.
4. European Union (EU27). European alternative fuels observatory. Published online July 15, 2025. https://alternative-fuels-observatory.ec.europa.eu/transport-mode/road/european-union-eu27.
5. Tong X. Hydrogen fuel cell vehicles for sustainable development in the automotive industry. Ali B, ed. *MATEC Web of Conferences*. 2024; 404: 01008. https://doi.org/10.1051/matecconf/202440401008.

6. Samsun R, Rex M, Antoni L, Stolten D. Deployment of fuel cell vehicles and hydrogen refueling station infrastructure: a global overview and perspectives. *Energies* 2022; 15(14): 14. https://doi.org/10.3390/en15144975.
7. IEA. Global EV outlook 2025. *Interational Energy Agency*. Published online 2025. https://www.iea.org/reports/global-ev-outlook-2025.
8. Kurc B, Gross X, Szymlet N, Rymaniak Ł, Woźniak K, Pigłowska M. Hydrogen-powered vehicles: a paradigm shift in sustainable transportation. *Energies* 2024; 17(19): 19. https://doi.org/10.3390/en17194768.
9. Szałek A, Pielecha I, Cieslik W. Fuel cell electric vehicle (FCEV) energy flow analysis in real driving conditions (RDC). *Energies* 2021; 14(16): 16. https://doi.org/10.3390/en14165018.
10. Samsun R, Rex M. *Deployment of fuel cell vehicles in road transport and the expansion of the hydrogen refueling station network 2023 Update*. Forschungszentrum Jülich GmbH, Zentralbibliothek, Verlag; 2023. https://doi.org/10.34734/FZJ-2023-03178.
11. H2 Station. Milestone reached: over 1,000 hydrogen refuelling stations in operation worldwide in 2024. Published online 2024. https://www.h2stations.org/press-releases.
12. Mahmood MA, Pérez De La Calle P, Meneses Zuluaga JM, Massarotti N, Sanchez-Diaz C. Techno-economic evaluation of hydrogen refuelling station with on-site electrolysis production powered by photovoltaic solar energy for the railway sector. *International Journal of Hydrogen Energy* 2025; 138: 802-822. https://doi.org/10.1016/j.ijhydene.2025.05.094.
13. Migliavacca G, Carlini C, Domenighini P, Zagano C. Hydrogen: prospects and criticalities for future development and analysis of present EU and national regulation. *Energies* 2024; 17(19): 19. https://doi.org/10.3390/en17194827.
14. Boretti AA. Energy recovery in passenger cars. *Journal of Energy Resources Technology* 2012; 134(2): 022203. https://doi.org/10.1115/1.4005699.
15. Carney D. Toyota unveils more new gasoline ICEs with 40% thermal efficiency. *SAE*. Published online April 4, 2018. https://www.sae.org/news/2018/04/toyota-unveils-more-new-gasoline-ices-with-40-thermal-efficiency?utm_source=chatgpt.com.
16. Dahham RY, Wei H, Pan J. Improving thermal efficiency of internal combustion engines: recent progress and remaining challenges. *Energies* 2022; 15(17): 6222. https://doi.org/10.3390/en15176222.
17. Mamala J, Tomczuk B, Waindok A, Graba M, Hennek K. Improving the efficiency of spark-ignition internal combustion engine using a novel electromagnetic actuator and adapting increased compression. *Energies* 2023; 16(14): 5355. https://doi.org/10.3390/en16145355.
18. Khalfan A, Andrews G, Li H. Real world driving: emissions in highly congested traffic. *SAE Technical Paper* 2017: 2017-01-2388. https://doi.org/10.4271/2017-01-2388.
19. Mamala J, Graba M, Prażnowski K, Hennek K. Control of the effective pressure in the cylinder of a spark-ignition engine by electromagnetic valve actuator. *SAE Technical Paper* 2019:2019-01-1201. https://doi.org/10.4271/2019-01-1201.
20. Serrano-Guevara ÓS, Huertas JI, Giraldo M. Real energy efficiency of road vehicles. *Energies* 2025; 18(8): 1933. https://doi.org/10.3390/en18081933.
21. Milojević S, Stopka O, Kontrec N, Orynycz O, Hlatká M, Radojković M, Stojanović B. Analytical characterization of thermal efficiency and emissions from a diesel engine using diesel and biodiesel and its significance for logistics management. *Processes* 2025; 13(7): 2124. https://doi.org/10.3390/pr13072124.
22. Rosero F, Fonseca N, López JM, Casanova J. Real-world fuel efficiency and emissions from an urban diesel bus engine under transient operating conditions. *Applied Energy* 2020; 261: 114442. https://doi.org/10.1016/j.apenergy.2019.114442.
23. Momen F, Rahman KM, Son Y, Savagian P. Electric motor design of general motors' Chevrolet Bolt electric vehicle. *SAE International Journal of Alternative Powertrains* 2016; 5(2): 286-293. https://doi.org/10.4271/2016-01-1228.
24. Paffumi E, De Gennaro M, Martini G, Manfredi U, Vianelli S, Ortenzi F, Genovese A. Experimental test campaign on a battery electric vehicle: on-road test results (Part 2). *SAE International Journal of Alternative Powertrains* 2015; 4(2): 277-292. https://doi.org/10.4271/2015-01-1166.
25. Parczewski K, Wnęk H. Analysis of energy flow in hybrid and electric-drive vehicles. *Energies* 2024; 17(8): 1915. https://doi.org/10.3390/en17081915.
26. Rosenberger N, Rosner P, Bilfinger P, Schöberl J, Teichert O, Schneider J, Abo Gamra K, Allgäuer C, Dietermann B, Schreiber M, Ank M, Kröger T, Köhler A, Lienkamp M. Quantifying the state of the art of electric powertrains in battery electric vehicles: comprehensive analysis of the Tesla Model 3 on the vehicle level. *World Electric Vehicle Journal* 2024; 15(6): 268. https://doi.org/10.3390/wevj15060268.

27. Rosenberger N. Vehicle parameter and electric powertrain efficiency analysis using real-driving data. *International Journal of Electrical and Electronic Engineering & Telecommunications* 2024; 13(6): 494-502. https://doi.org/10.18178/ijeetc.13.6.494-502.
28. Lohse-Busch H, Stutenberg K, Duoba M, Liu X, Elgowainy A, Wang M, Wallner T, Richard B, Christenson M. Automotive fuel cell stack and system efficiency and fuel consumption based on vehicle testing on a chassis dynamometer at minus 18 °C to positive 35 °C temperatures. *International Journal of Hydrogen Energy* 2020; 45(1): 1. https://doi.org/10.1016/j.ijhydene.2019.10.150.
29. Sery J, Leduc P. Fuel cell behavior and energy balance on board a Hyundai Nexo. *International Journal of Engine Research* 2022; 23(5): 709-720. https://doi.org/10.1177/14680874211059046.
30. Najjar YSH. Hydrogen safety: the road toward green technology. *International Journal of Hydrogen Energy* 2013; 38(25): 10716-10728. https://doi.org/10.1016/j.ijhydene.2013.05.126.
31. Manzo D, Thai R, Le HT, Venayagamoorthy GK. Fuel cell technology review: types, economy, applications, and vehicle-to-grid scheme. *Sustainable Energy Technologies and Assessments* 2025; 75: 104229. https://doi.org/10.1016/j.seta.2025.104229.
32. Legala A, Kubesh M, Chundru VR, Conway G, Li X. Machine learning modeling for fuel cell-battery hybrid power system dynamics in a Toyota Mirai 2 vehicle under various drive cycles. *Energy and AI* 2024; 17: 100415. https://doi.org/10.1016/j.egyai.2024.100415.
33. Matsunaga M, Fukushima T, Ojima K. Powertrain system of Honda FCX Clarity fuel cell vehicle. *World Electric Vehicle Journal* 2009; 3(4): 820-829. https://doi.org/10.3390/wevj3040820.
34. Wang Y, Yuan H, Martinez A, Hong P, Xu H, Bockmiller FR. Polymer electrolyte membrane fuel cell and hydrogen station networks for automobiles: status, technology, and perspectives. *Advances in Applied Energy* 2021; 2: 100011. https://doi.org/10.1016/j.adapen.2021.100011.
35. Konno N, Mizuno S, Nakaji H, Ishikawa Y. Development of compact and high-performance fuel cell stack. *SAE International Journal of Alternative Powertrains* 2015; 4(1): 123-129. https://doi.org/10.4271/2015-01-1175.
36. Yoshizumi T, Kubo H, Okumura M. Development of high-performance FC stack for the New MIRAI. SAE Technical Paper 2021:2021-01-0740. https://doi.org/10.4271/2021-01-0740.
37. Hong BK, Kim SH. Recent advances in fuel cell electric vehicle technologies of Hyundai. *ECS Transactions* 2018; 86(13): 3-11. https://doi.org/10.1149/08613.0003ecst.
38. Von Tettau P, Sterlepper S, Mauermann P, Wick M, Tinz S, Jesser M, Walters M, Pischinger S. Laboratory assessments applied to mass-produced automotive fuel cells. *International Journal of Hydrogen Energy* 2024; 52: 1127-1136. https://doi.org/10.1016/j.ijhydene.2023.10.309.
39. Kimura K, Kawasaki T, Ohmura T, Atsumi Y, Shimizu K. Development of new fuel cell vehicle Clarity Fuel Cell. *Honda R&D Technical Review*. Published online April 2016.
40. Liu S, Yuan S, Liang Y, Li H, Xu Z, Xu Q, Yin J, Shen S, Yan X, Zhang J. Engineering the catalyst layers towards enhanced local oxygen transport of low-Pt proton exchange membrane fuel cells: materials, designs, and methods. *International Journal of Hydrogen Energy* 2023; 48(11): 4389-4417. https://doi.org/10.1016/j.ijhydene.2022.10.249.
41. Wang Y, Ruiz Diaz DF, Chen KS, Wang Z, Adroher XC. Materials, technological status, and fundamentals of PEM fuel cells – a review. *Materials Today* 2020; 32: 178-203. https://doi.org/10.1016/j.mattod.2019.06.005.
42. Takahashi T, Ikeda T, Murata K, Hotaka O, Hasegawa S, Tachikawa Y, Nishihara M, Matsuda J, Kitahara T, Lyth SM, Hayashi A, Sasaki K. Accelerated durability testing of fuel cell stacks for commercial automotive applications: a case study. *Journal of The Electrochemical Society* 2022; 169(4): 044523. https://doi.org/10.1149/1945-7111/ac662d.
43. Andrade TS, Thiringer T. Low platinum fuel cell as enabler for the hydrogen fuel cell vehicle. *Journal of Power Sources* 2024; 598: 234140. https://doi.org/10.1016/j.jpowsour.2024.234140.
44. Borup RL, Kusoglu A, Neyerlin KC, Mukundan R, Ahluwalia RK, Cullen DA, More KL, Weber AZ, Myers DJ. Recent developments in catalyst-related PEM fuel cell durability. *Current Opinion in Electrochemistry* 2020; 21: 192-200. https://doi.org/10.1016/j.coelec.2020.02.007.
45. Osmieri L, Park J, Cullen DA, Zelenay P, Myers DJ, Neyerlin KC. Status and challenges for the application of platinum group metal-free catalysts in proton-exchange membrane fuel cells. *Current Opinion in Electrochemistry* 2021; 25: 100627. https://doi.org/10.1016/j.coelec.2020.08.009.

46. Fuel Cell Standards Committee. Recommended Practice for Measuring Fuel Consumption and Range of Fuel Cell and Hybrid Fuel Cell Vehicles Fuelled by Compressed Gaseous Hydrogen. https://doi.org/10.4271/J2572_201410.
47. ISO 23828:2022. Fuel cell road vehicles — Energy consumption measurement — Vehicles fuelled with compressed hydrogen. *ISO*. Published online 2022. Accessed July 21, 2025. https://www.iso.org/standard/78416.html.
48. Alves BM, Savignac P, Leduc P. Energy balance and hydrogen exhaust emissions of the second-generation Toyota Mirai. *International Journal of Hydrogen Energy* 2025; 156: 150411. https://doi.org/10.1016/j.ijhydene.2025.150411.
49. UN Regulation No 154. Uniform provisions concerning the approval of light duty passenger and commercial vehicles with regards to criteria emissions, emissions of carbon dioxide and fuel consumption and/or the measurement of electric energy consumption and electric range (WLTP) [2021/2039]. Published online 2021.
50. Duan Z, Zhang L, Feng L, Yu S, Jiang Z, Xu X, Hong J. Research on economic and operating characteristics of hydrogen fuel cell cars based on real vehicle tests. *Energies* 2021; 14(23): 7856. https://doi.org/10.3390/en14237856.
51. Pielecha I, Szwajca F. Experimental study and modelling of an air-cooled proton exchange membrane fuel cell stack in the static and dynamic performance. *Eksploatacja i Niezawodność – Maintenance and Reliability* 2024; 26(2). https://doi.org/10.17531/ein/184232.
52. Tan P, Xu L, Fang L, Zhuang C, Jiang Z, Lou D, Zhang Y, Hu Z. Energy analysis and efficiency optimization of a fuel cell passenger vehicle based on energy flow distribution and thermal management under various driving conditions. *Energy* 2025; 340: 139003. https://doi.org/10.1016/j.energy.2025.139003.
53. Li S, Sang X, Zhu Z, Jiang W, Wang W, Li C, Wang X.. Parametric analysis and energy efficiency optimization control of integrated thermal management system with waste heat utilization for fuel cell vehicles. *International Journal of Hydrogen Energy* 2026; 204: 153037. https://doi.org/10.1016/j.ijhydene.2025.153037.
54. Dicks AL, Rand DAJ. *Fuel Cell Systems Explained*. 1st ed. Wiley; 2018. https://doi.org/10.1002/9781118706992.
55. Pielecha I. Modeling of fuel cells characteristics in relation to real driving conditions of FCHEV vehicles. *Energies* 2022; 15(18): 6753. https://doi.org/10.3390/en15186753.
56. Pielecha I, Szałek A, Tchorek G. Two generations of hydrogen powertrain – an analysis of the operational indicators in real driving conditions (RDC). *Energies* 2022; 15(13): 4734. https://doi.org/10.3390/en15134734.